

COVID-19 data sharing and collaboration

DOMINIQUE DUNCAN*

There is an immediate need to study COVID-19, and the COVID-19 Data Archive (COVID-ARC) provides access to data along with user-friendly tools for researchers to perform analyses to better understand COVID-19 and encourage collaboration on this research. The COVID-19 pandemic has been spreading rapidly across the world, and there are still many unknowns about COVID-19. There is an urgent need for scientists around the world to work together to model the virus, study how the virus has changed and will change over time, understand how it spreads, and study transmission after vaccination. COVID-ARC can also prepare scientists for future pandemics by putting the infrastructure in place to enable researchers to aggregate data and perform analyses quickly in the event of an emergency. We have developed a platform of networked and centralized web-accessible data archives to store multimodal data related to COVID-19 and make them broadly available and accessible to the world-wide scientific community to expedite research in this area. COVID-ARC provides tools for researchers to visualize and analyze various types of data as well as a website with tools for training, announcements, virtual information sessions, and a knowledgebase wherein researchers post questions and receive answers from the community.

KEYWORDS AND PHRASES: Informatics, datasets, harmonization, image segmentation, COVID-19, archive, machine learning, data analysis.

1. Introduction

The COVID-19 Data Archive (COVID-ARC), developed at the University of Southern California (USC) Laboratory of Neuro Imaging (LONI), is a platform of networked and centralized web-accessible data archives to store and curate multimodal data related to coronavirus disease 2019 (COVID-19). Public datasets have been made broadly available and accessible to

*Joint work with Alexis Bennett, Alexander Bruckhaus, Aksh Garg, Rachael Garner, Azrin Khan, Marianna La Rocca, Jiaju Liu, Aubrey Martinez, Noor Nouaili, Sana Salehi, and Yujia Zhang.

the world-wide scientific community, and private datasets are available by request and approval of the data provider. We have provided links and instructions for how to request access to these private datasets to help facilitate the process between users who wish to request access to the data and the data providers who will make the decision regarding granting access. The goal of this archive is to expedite research on COVID-19 due to the urgent nature of this pandemic. COVID-ARC data include or will soon include symptoms, vitals, demographic, geolocation, chest computed tomography (CT), X-ray, ultrasound, brain magnetic resonance imaging (MRI), and electroencephalography (EEG) of COVID-19 patients. There is an immediate need to model and understand the spread of COVID-19, and this archive aims to provide access to data and user-friendly tools for researchers to perform analyses to better understand COVID-19 and encourage collaboration on this research. We have built this informatics system, leveraging our previous work in developing data repositories [1, 2], to provide an efficient, secure, HIPAA-compliant data repository platform that facilitates data de-identification, quality control, aggregation, visualization, integrated processing, download, and training. As we have developed this data archive and worked to curate and harmonize data from different sites, equipment, and protocols so that the data can be analyzed across various data collection sites, we have been analyzing these data and sharing both the analytic tools and resulting processed data on COVID-ARC for the broader COVID-19 research community.

Visualizing data helps orient researchers so that they can inspect and compare data, and it provides contextual information to model COVID-19 and study the outcomes and spread. Users have access to pipeline workflows, containing a variety of statistical and analytic tools that have proven to be effective in other studies, such as in our Data Archive for the BRAIN Initiative (DABI) at LONI. The LONI Pipeline [3–5] can utilize processing modules from any software suite, allowing integration of tools developed by outside researchers in various programming languages. After requesting a free account, users are able to search across datasets and perform analyses directly on the LONI server so that users do not need to download data locally to their computers. Furthermore, researchers are able to upload their own algorithms and analytic tools that may be used on COVID-ARC data and shared with others. Users can share preliminary results and form discussions that may lead to new collaborations on the COVID-ARC website (<https://covid-arc.loni.usc.edu>). The website also has information about recent news and events, including recordings from webinars that the COVID-ARC team has participated in or hosted, some of which involve K-12

students and teachers. COVID-ARC is providing opportunities for training and outreach via webinars with lightning talks and panel sessions as well as virtual training sessions for interested researchers to use the resources and central, web-based tools that link our collaborative research community.

With the growing number of multimodal datasets that have been aggregated in COVID-ARC, and the 18PB of storage capacity at LONI, we have applied machine learning methods and developed new analytic tools, augmenting our existing tools, to classify COVID-19 positive and negative patients, extract the most important imaging features to identify COVID-19, and predict severity of the disease. If we are able to identify various key features of COVID-19, we may be able to treat those patients who are most at risk in the future to minimize their symptoms or help prevent some long-term effects.

There is evidence that chest CT imaging has a high sensitivity for COVID-19 diagnosis and may be more sensitive than the viral test, so it should be considered as a primary tool for detection [6, 7]. Many studies have analyzed CT and follow-up CT scans of COVID-19 patients [6, 8–25] as well as X-ray [26–29] and positron emission tomography (PET) [30–33]. However, there is a lack of rigorous studies that perform image analysis linked to clinical or laboratory findings, and COVID-ARC encourages data fusion, because it is likely that we will not understand COVID-19 well enough by studying just one data type.

2. Imaging data

COVID-ARC has aggregated and curated 19 COVID-19 imaging and 4 other multimodal datasets for publicly available download. These datasets include X-ray, CT, and ultrasound images collected from international institutions, including Tongji Hospital of Wuhan, China; Italian Society of Medical and Interventional Radiology, Italy; Wenzhou Medical University, China; Valencian Region Medical ImageBank, Spain; Moscow Center of Diagnostics and Telemedicine, Russia; Negin Medical Center, Iran; University of Montreal, Canada; and Institute for Diagnostic and Interventional Radiology, Germany. Additional datasets aggregate patients from various regional hubs, including Sao Paulo in Brazil, Netanya in Israel, South Korea, and numerous American hospitals.

Images are stored as NIFTI, PNG, TGZ, and TIF file formats and include:

- 264,976 COVID-19 positive images
- 350,578 COVID-19 negative images (including both healthy controls and common pneumonia patients)

Available data are summarized in Figure 1. COVID-ARC has integrated Aspera [34], a Health Insurance Portability and Accountability Act (HIPAA)-compliant, encrypted, high-speed file transfer system from IBM, to support and facilitate new dataset upload.

3. Data ingestion and preprocessing

Once data are centrally stored in COVID-ARC, data undergo harmonization and quality control to facilitate standardized analysis. Metadata, including demographics, outcome, and clinical measures of severity, are harmonized and validated by a medical doctor who specializes in radiology. Once completed, harmonized metadata and quality control reports of images are made available to users. We have been performing quality control [35] on all COVID-ARC images and attaching files with good, questionable, and poor labels to make these available for all COVID-ARC users. For questionable images, we are providing filters, some of which we have developed at LONI for neuroimaging and are adapting to these data, to improve image quality so these data can be usable for analysis.

4. Image segmentation

Using COVID-ARC, we have performed lung and infection segmentation to generate lung masks and segmented infections (Figure 2). Infection segmentations allow for quantification of potentially pathologic findings, including consolidation, ground glass opacities, and crazy paving patterns [36]. Future work will include evaluation of the relationship between the infection findings, including size, type, and lobular involvement, with COVID-19 positivity. Such results may allow for imaging findings to be used as a rapid precursory diagnostic tool, as CT and X-ray are faster to acquire than polymerase chain reaction (PCR) testing. To date, 264,976 COVID-19 positive and 350,745 COVID-19 negative lung masks, segmented images, and infection masks are available for download.

We are exploring more efficient and semi-automatic, threshold-based methods to generate accurate infection segmentations, as manual segmentation requires significant radiological and clinical expertise and is time-intensive. A binarized threshold combined with Region Adjacency Graph

DIRECTORY FILE STRUCTURE

covid-19/arc
Text file listing each dataset with its assigned ID number used throughout the project

* Each site has a Quality Control (QC) file listing images that may require review due to low quality
* Each site has an ID-mapping file that maps the file names on the COVID-ARC server to that of the original datasets

DATA STRUCTURE	Location	Modality	File Format	Metadata	Number of Images		Number of Patients		Public		
					COVID-19	Non-COVID-19	COVID-19	Non-COVID-19			
Original data aggregated from various sites	Site 1	Sao Paulo, Brazil	CT	png		2168	Other pulmonary illnesses: 247 Healthy: 718	80	Other pulmonary illnesses: 80 Healthy: 50	Yes	
	Site 2	China	CT	png	Patient details including age, sex, city, medical history, time of scan, CT scan abnormalities, and comorbidities	349	463	216	55	Yes	
	Site 3	Italy	CT	ni	Patient details including age, sex, clinical symptoms, hospital, medical history, and CT scan abnormalities and comorbidities	110		60		Yes	
	Site 4	Wenzhou, China and Netanya, Israel	CT	ni	Includes hospitals where images were acquired	20				Yes	
	Site 5	Valencian Region Medical Bank	CT	tgtz		CT 900 X-Ray 16800				Yes	
	Site 6	Moscow, Russia	CT	ni	Patients are split into 5 categories based on severity of disease	1110		1110		Yes	
	Site 7	Sari, Iran	CT	tif	Patient details including age, sex, diagnosis, date of scan, and location of scan	15589	48260	95	282	Subset for Machine Learning	Yes
						2282	9776	95	282		
	Site 8	Various locations	X-Ray	png	Patient details including age, sex, diagnosis, severity/modality, date of scan, and location of scan abnormalities and comorbidities	CT 84 X-Ray 857					Yes
	Site 9	University of Electronic Science & Technology, China	CT	ni		120		120			No
	Site 10	China Consortium of Chest CT Image	CT	png	Patient details including age, sex, critical illness, liver function, lung function, and time of progression	159702	Pneumonia 150071 Normal 95756	488	*Patient group not specified		Yes
	Site 11	Hannover, Germany	X-Ray	ni	Patient details including age, sex, time of progression, and clinical findings. Age, size, and weight will be published in the future	343					Yes
	Site 12	Various locations	X-Ray	png	Patient details including age, sex, time of progression, and clinical findings. Age, size, and weight will be published in the future	219	Viral Pneumonia 1345 Normal 1341				Yes
	Site 13	Spain	None available	csv	Patient details including age, sex, diagnosis, progression of disease, lab results, treatment, and death ascertainment						No
	Site 14	Various locations	None available	csv	Daily levels of COVID-19 cases, recoveries, and deaths worldwide						Yes
	Site 15	South Korea	None available	csv	Patient epidemiological data, time series data, and regional data based on affected cases						Yes
	Site 16	Various locations	Ultrasound	Videos .gif img, mp4 Images .png, .jpg	Patient details including diagnosis, symptoms, age, sex, and lung abnormalities. Image details including frame rate, frame length, and resolution	50	57	73		Bacterial/Viral Pneumonia Healthy	Yes
						Images 22	22	15			
	Site 17	Radiological Society of North America	CT	ni		632		632			Yes
	Site 18	Arkansas, USA	CT, DX, X-Ray	dom	Patient details including age, weight, height, race, sex, comorbidities, lab data, and patient outcome	31,935		105			Yes
	Site 19	Radiological Society of North America	CT	dom		31,856		110			Yes
	Site 20	Radiological Society of North America	X-Ray	dom				30,000			Yes
	Site 21	Guangzhou, China	X-Ray	jpg				Pneumonia 4,273 Normal 1,583			Yes
Site 22	Los Angeles, CA									No	
Site 23	Various locations	None available	csv	Neurological complications accompanying COVID-19 as well as demographic information of patients		581				Yes	

	Location	Available Analysis	File Format	Number of Images		Number of Patients		
				COVID-19	Non-COVID-19	COVID-19	Non-COVID-19	
ANALYSIS STRUCTURE Image Processing Outputs	Site 1	Sao Paulo, Brazil	Lung masks	ni	1248	1219		
			Segmented images	png	1252	1199		
	Site 2	China	Lung masks	png	349	463	216	44
	Site 3	Italy	COVID-19 masks	ni	110		60	
			Lung masks	ni	110		60	
	Site 4	Wenzhou, China and Netanya, Israel	COVID-19 masks	ni	20		20	
			Lung masks	ni	20		20	
	Site 5	Valencian Region Medical Bank	Lung + COVID-19 masks	ni	20		20	
			Annotated COVID-19 masks	tgtz	23		20	
	Site 6	Moscow, Russia	COVID-19 masks	ni	50		50	
	Site 7	Sari, Iran	None Available					
	Site 8	Various locations	Lung masks	png				
	Site 9	University of Electronic Science and Technology, China	Annotated COVID-19 masks	ni	120		120	
	Site 10	China Consortium of Chest CT Image Investigation	COVID-19 masks	ni	750		150	
	Site 11	Hannover, Germany	None Available					
	Site 12	Various Locations	None Available					
	Site 13	Spain	None Available					
	Site 14	South Korea	None Available					
	Site 15	Various Locations	None Available					
	Site 16	Various Locations	None Available					
	Site 17	Radiological Society of North America	Detailed annotation	json				
	Site 18	Little Rock, Arkansas	Detailed annotation	json				
	Site 19	Radiological Society of North America	Detailed annotation	json				
Site 20	Radiological Society of North America	None Available						
Site 21	Guangzhou, China	None Available						
Site 22	Los Angeles, CA	None Available						
Site 23	Various locations	None Available						

Figure 1: An overview of data stored in COVID-ARC. Available data include imaging (CT, X-ray, ultrasound), harmonized metadata, and analysis. Analysis outputs include lung masks and infection segmentations.

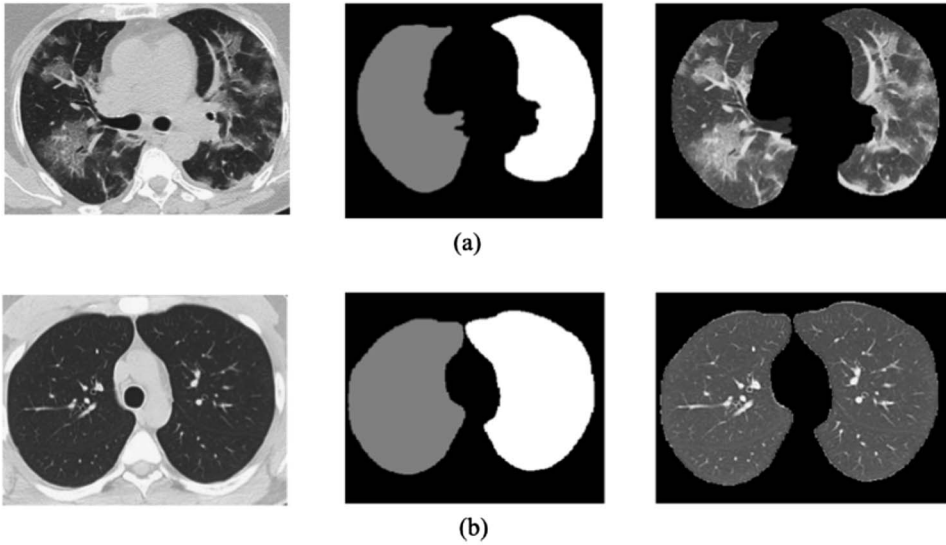


Figure 2: Examples of lung mask segmentation generated using the Lung Mask tool [37] for (a) COVID-19 positive and (b) COVID-19 negative patients.

method has shown promise in automatically segmenting infected regions and generating infection rates. The proposed method calculates infection rate within $\pm 2\%$ of ground truth segmentations (Figure 3). Thus, this could be a potentially useful tool for radiologists to accurately assess infection severity and analyze disease progression in follow-up CT scans.

5. Machine learning applied to CT images

In addition to aggregating, standardizing, and segmenting data, we have begun performing analysis on stored datasets and sharing preliminary findings on COVID-ARC. We are applying machine learning and deep learning methods to imaging data to identify COVID-19 positive subjects accurately with an automated method. After training 40 models on a dataset of CT images from Sao Paulo, Brazil, including both base models and modified networks, novel machine learning pipelines using EfficientNet architectures were found to have greater than 99% accuracy. Introduction of innovative visualization using Gradient-weighted Class Activation Mapping has also demonstrated that the architecture effectively utilizes regions of infection to classify subjects (Figure 4).

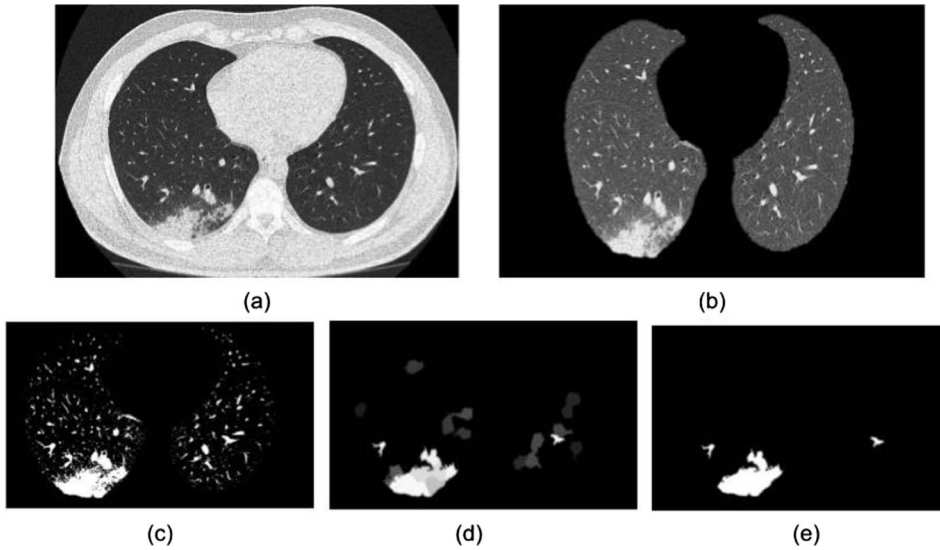


Figure 3: Images representing sequential stages of the threshold-based segmentation method to quantify COVID-19 lung infection: (a) original CT slice, (b) 2D segmented lungs, (c) implemented binary thresholding, (d) implemented region adjacency graph thresholding, and (e) additional thresholding, which may be used to compute the hyperintensity density of segmented regions to compare with the total mask pixel density.

Furthermore, we have applied transfer learning and evaluated 6 pre-trained convolutional neural network (CNN) models on one dataset to compare their ability to classify COVID-19 patients from chest CT images. Transfer learning that utilizes a pretrained CNN model has shown promise in this COVID-19 application: a pretrained InceptionV3 Model yielded 98.71% accuracy when applied to a dataset of 489 subjects from Sao Paulo, Brazil (Figure 5). Data were split into 80% for training and 20% for validation. Each model was trained and tested using 5 rounds of cross validation on augmented segmented and non-segmented training classes; we found that training on segmented images is statistically comparable to training on non-segmented images.

Deep learning is a promising, low-cost, and reliable way to determine if patients are infected with COVID-19 from examining their lung CT scans. However, the currently popular CNNs risk overfitting to hospital-specific data due to the lack of publicly available CT data. We have tested the performance of Siamese neural networks (SNNs) [38], networks that learn

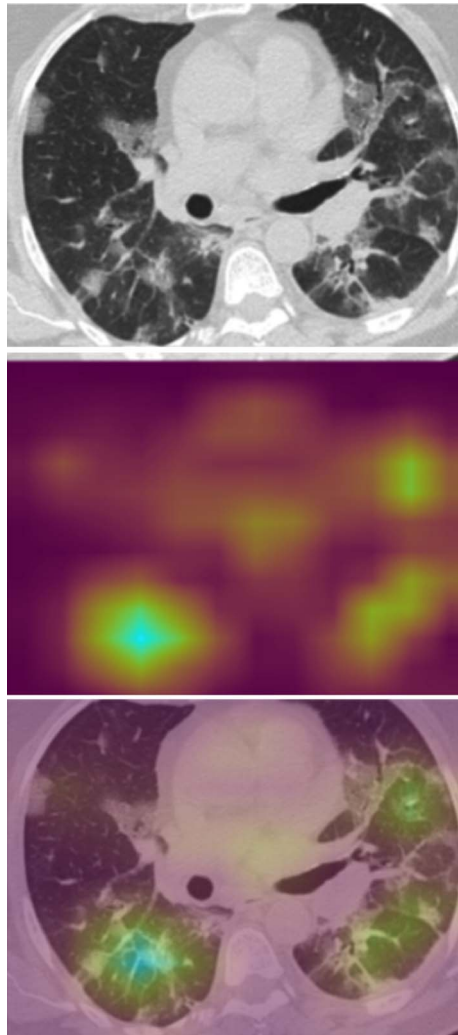


Figure 4: Gradient-weighted Class Activation Map (Grad-CAM) produced for one COVID-19 subject. Grad-CAMs increase model interpretability by visualizing the important regions in the image to predict COVID-19 positivity. The blue/green regions represent more important regions, and the purple/red represent less important regions. If overlaid onto the original CT scan, the important regions correspond to areas of higher ground glass opacities and crazy paving patterns, two potential findings that have been found to be present in COVID-19 subjects.

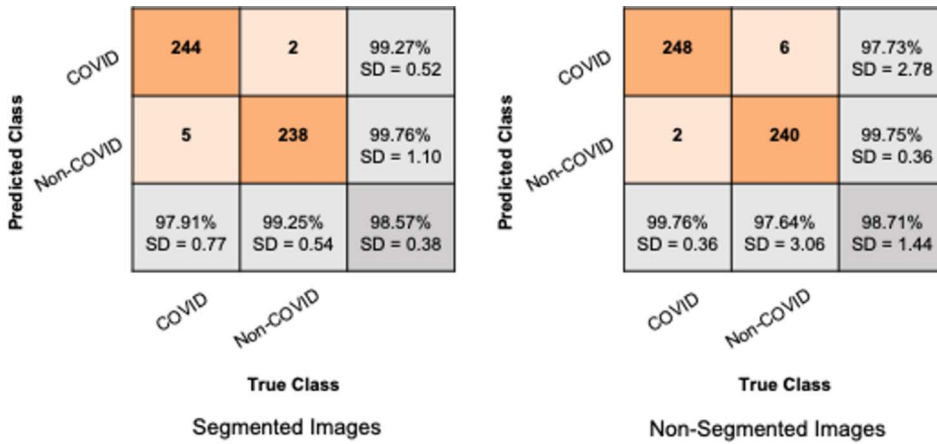


Figure 5: Confusion matrices for COVID-19 detection on 489 subjects using an InceptionV3 transfer learning-based architecture. Classification was performed using both segmented images, in which lungs were first segmented from CT, and non-segmented images. Both classifications yielded greater than 98% accuracy.

to determine the similarity between two images rather than label them as COVID-19 positive or negative. SNNs have previously demonstrated state-of-the-art performance even when applied to test data that bear little resemblance to their training data. We trained 4 different SNNs on CT images collected from Sari, Iran. Our models achieved higher accuracy than current models and lay the groundwork for creating a model that correctly discriminates COVID-19 positive and negative CT images collected from any hospital.

Saliency Maps (Figure 6) highlighted potentially novel patterns and locations in the lower lobes that are related to COVID-19 infection. SNNs are useful for tasks where labeled data are difficult to acquire, as is the case with many COVID-19 imaging datasets, so SNNs may be a promising tool for clinicians to use machine learning methods to diagnose patients using CT images while only having a small number of reference images at their hospital.

6. Correlational analysis

In addition to image analysis, we have performed correlational analysis on other data from COVID-ARC. Demographic correlational analyses have begun to uncover relationships between racial and gender identity, smoking

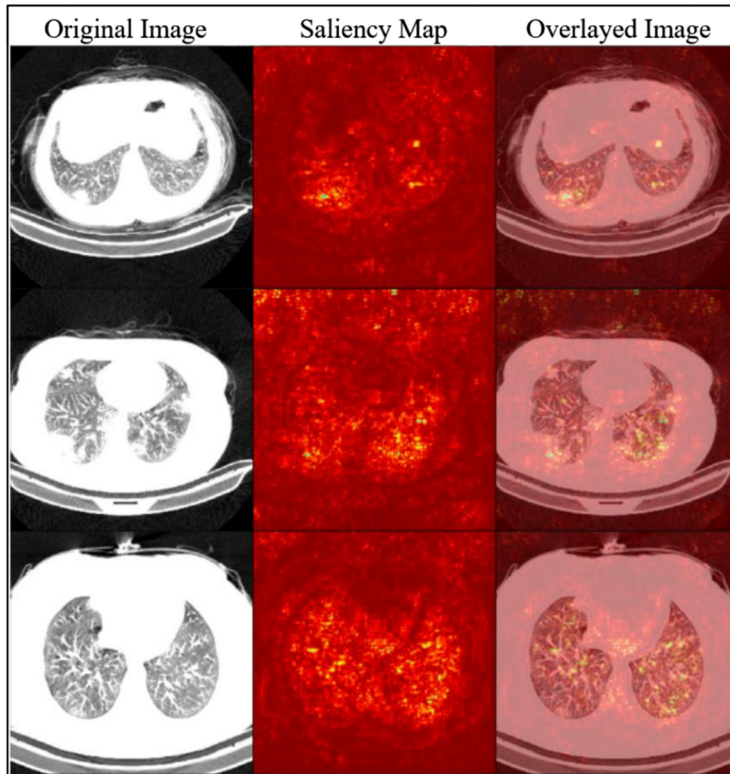


Figure 6: Saliency maps generated of two COVID-19 positive patients (top, middle) and one COVID-19 negative patient (bottom).

habits, and blood type as well as rates of COVID-19 infection and severity of disease. An exhaustive search of United States data has also elucidated relationships between infection rates and mask requirements, political affiliation, and local business restrictions. A significant increase in infection rates was found 2 weeks after partial or full reopening of business in 83 United States counties with more than 20,000 COVID-19 cases as of November 2020. Infection rates were compared before and after reopening of various public businesses including restaurants, bars, retail, gyms, salons/barbers, and public schools. Among partially reopened businesses, bars were associated with the highest change of infection rate (Figure 7), and among fully opened businesses, gyms were associated with the highest change of infection rate. This research provides insight into the transmission of COVID-19 and promotes evidence-driven policymaking for disease prevention and community health.

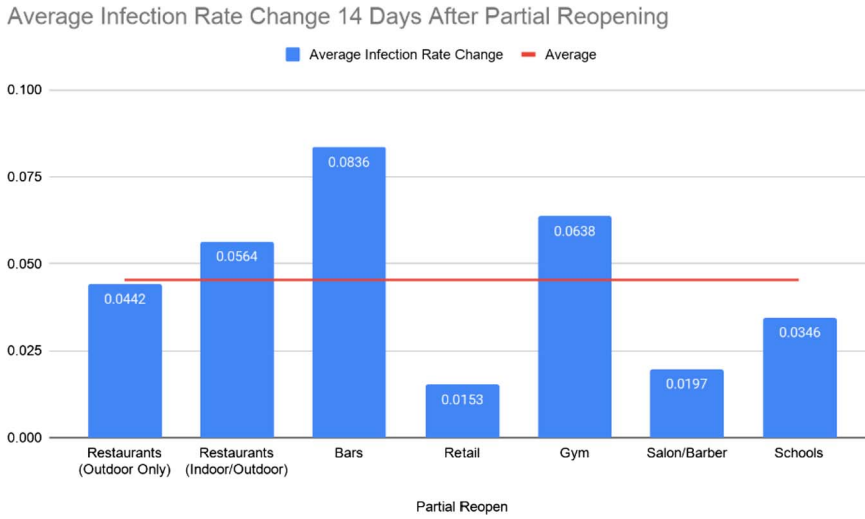


Figure 7: The average 14-day change of infection for each respective partially reopened business. The red line indicates the average change of infection rate among all businesses.

7. Discussion and future work

COVID-ARC provides researchers around the world a multimodal data archive of publicly available datasets as well as instructions to request access to private datasets related to COVID-19. Besides data access, COVID-ARC also provides a variety of tools that we have previously developed in addition to innovative methods that we are currently developing for this project. The website includes a knowledgebase to encourage researchers from different hospitals and universities to work together to provide an efficient way to understand COVID-19. Not only does this archive and associated quality control, visualization, and analytic tools help expedite COVID-19 research and facilitate international collaboration, but this archive will prepare us for the next pandemic so that we will have the infrastructure in place to enable researchers to aggregate data and perform analyses quickly at the onset of the next pandemic. We have performed lung and infection segmentation to generate lung masks and segmented infections to help researchers with their COVID-19 image analyses. Moreover, we have performed a variety of analyses, focusing mainly on imaging data, to identify COVID-19 positive and negative patients with high accuracy. Several examples of preliminary findings using COVID-ARC machine learning analysis as well as correlational analysis have been described. Future work will include continuing the

aforementioned analyses on more datasets and improving the accuracy of our methods in addition to studying neurological effects of COVID-19 by analyzing neuroimaging data. We will continue to share both our methods and resulting analyses along with up-to-date aggregated datasets on COVID-ARC with the goal to expedite COVID-19 research during this global pandemic.

Acknowledgments

This work was supported by the National Science Foundation under Award Number 2027456 (COVID-ARC).

References

- [1] D. Duncan, P. Vespa, A. Pitkänen, A. Braimah, N. Lapinlampi, A. W. Toga, Big data sharing and analysis to advance research in post-traumatic epilepsy. *Neurobiology of Disease* **123** (2019), 127–136.
- [2] D. Duncan, G. Barisano, R. Cabeen, F. Sepehrband, R. Garner, A. Braimah, P. Vespa, A. Pitkänen, M. Law, A. W. Toga, Analytic tools for post-traumatic epileptogenesis biomarker search in multimodal dataset of an animal model and human patients. *Frontiers in Neuroinformatics* **12** (2018), 86.
- [3] I. D. Dinov, F. Torri, F. Macchiardi, P. Petrosyan, Z. Liu, A. Zamanyan, P. Eggert, J. Pierce, A. Genco, J. A. Knowles, A. P. Clark, J. D. Van Horn, J. Ames, C. Kesselman, A. W. Toga, Applications of the pipeline environment for visual informatics and genomics computations. *BMC Bioinformatics* **12.1** (2011), 1–20.
- [4] I. D. Dinov, J. D. Van Horn, K. M. Lozev, R. Magsipoc, P. Petrosyan, Z. Liu, A. MacKenzie-Graham, P. Eggert, D. S. Parker, A. W. Toga, Efficient, distributed and interactive neuroimaging data analysis using the LONI Pipeline. *Frontiers in Neuroinformatics* **3** (2009), 22.
- [5] A. J. MacKenzie-Graham, A. Payan, I. D. Dinov, J. D. Van Horn, A. W. Toga, Neuroimaging data provenance using the LONI pipeline workflow environment. *International Provenance and Annotation Workshop*. Springer, Berlin, Heidelberg (2008), 208–220.
- [6] T. Ai, Z. Yang, H. Hou, C. Zhan, C. Chen, W. Lv, Q. Tao, Z. Sun, L. Xia, Correlation of chest CT and RT-PCR testing in coronavirus disease 2019 (COVID-19) in China: A report of 1014 cases. *Radiology* **296.2** (2020), E32–40.

- [7] S. Salehi, A. Abedi, S. Balakrishnan, A. Gholamrezanezhad, Coronavirus disease 2019 (COVID-19): a systematic review of imaging findings in 919 patients. *American Journal of Roentgenology* **215.1** (2020), 87–93.
- [8] H. Shi, X. Han, N. Jiang, Y. Cao, O. Alwalid, J. Gu, Y. Fan, C. Zheng, Radiological findings from 81 patients with COVID-19 pneumonia in Wuhan, China: a descriptive study. *The Lancet Infectious Diseases* **20.4** (2020), 425–434.
- [9] W. Zhao, Z. Zhong, X. Xie, Q. Yu, J. Liu, Relation between chest CT findings and clinical conditions of coronavirus disease (COVID-19) pneumonia: a multicenter study. *American Journal of Roentgenology* **214.5** (2020), 1072–1077.
- [10] A. Bernheim, X. Mei, M. Huang, Y. Yang, Z. A. Fayad, N. Zhang, K. Diao, B. Lin, X. Zhu, K. Li, S. Li, H. Shan, A. Jacobi, M. Chung, Chest CT findings in coronavirus disease-19 (COVID-19): relationship to duration of infection. *Radiology* (2020), 200463.
- [11] J. Wang, J. Liu, Y. Wang, W. Liu, X. Chen, C. Sun, X. Shen, Q. Wang, Y. Wu, W. Liang, L. Ruan, Dynamic changes of chest CT imaging in patients with COVID-19. *Journal of Zhejiang University (Medical Sciences)* **49.2** (2020), 191–197.
- [12] W. Yang, Q. Cao, L. E. Qin, X. Wang, Z. Cheng, A. Pan, J. Dai, Q. Sun, F. Zhao, J. Qu, F. Yan, Clinical characteristics and imaging manifestations of the 2019 novel coronavirus disease (COVID-19): a multicenter study in Wenzhou city, Zhejiang, China. *Journal of Infection* **80.4** (2020), 388–393.
- [13] X. Li, X. Zeng, B. Liu, Y. Yu, COVID-19 infection presenting with CT halo sign. *Radiology: Cardiothoracic Imaging* **2.1** (2020), e200026.
- [14] W. Zhang, Imaging changes in severe COVID-19 pneumonia. *Intensive Care Medicine* **46.4** (2020), 583–585.
- [15] D. Dong, Z. Tang, S. Wang, H. Hui, L. Gong, Y. Lu, Z. Xue, H. Liao, F. Chen, F. Yang, R. Jin, The role of imaging in the detection and management of COVID-19: a review. *IEEE Reviews in Biomedical Engineering* (2020). [MR4035999](#)
- [16] Z. Z. Jiang, C. He, D. Q. Wang, H. L. Shen, J. L. Sun, W. N. Gan, J. Y. Lu, X. T. Liu, The role of imaging techniques in management of

- COVID-19 in China: from diagnosis to monitoring and follow-up. *Medical Science Monitor: International Medical Journal of Experimental and Clinical Research* **26** (2020), e924582–1.
- [17] R. Aljondi, S. Alghamdi, Diagnostic value of imaging modalities for COVID-19: scoping review. *Journal of Medical Internet Research* **22.8** (2020), e19673.
- [18] W. J. Guan, Z. Y. Ni, Y. Hu, W. H. Liang, C. Q. Ou, J. X. He, L. Liu, H. Shan, C. L. Lei, D. S. Hui, B. Du, China medical treatment expert group for COVID-19. *Clinical Characteristics of Coronavirus Disease* (2019), 1708–1720.
- [19] F. Pan, T. Ye, P. Sun, S. Gui, B. Liang, L. Li, D. Zheng, J. Wang, R. L. Hesketh, L. Yang, C. Zheng, Time course of lung changes at chest CT during recovery from coronavirus disease 2019 (COVID-19). *Radiology* **295.3** (2020), 715–721.
- [20] J. Wu, C. L. Feng, X. Y. Xian, J. Qiang, J. Zhang, Q. X. Mao, S. F. Kong, Y. C. Chen, J. P. Pan, Novel coronavirus pneumonia (COVID-19) CT distribution and sign features. *Chinese Journal of Tuberculosis and Respiratory Diseases* **43** (2020), E030.
- [21] H. X. Bai, B. Hsieh, Z. Xiong, K. Halsey, J. W. Choi, T. M. Tran, I. Pan, L. B. Shi, D. C. Wang, J. Mei, X. L. Jiang, Performance of radiologists in differentiating COVID-19 from non-COVID-19 viral pneumonia on chest CT. *Radiology* **296.2** (2020), E46–E54.
- [22] Z. W. Zhu, J. J. Tang, X. P. Chai, Z. F. Fang, Q. M. Liu, X. Q. Hu, D. Y. Xu, L. Tang, S. Tai, Y. Z. Wu, S. H. Zhou, Comparison of heart failure and 2019 novel coronavirus pneumonia in chest CT features and clinical characteristics. *Zhonghua xin xue Guan Bing za zhi* **48** (2020), E007.
- [23] H. Chen, J. Guo, C. Wang, F. Luo, X. Yu, W. Zhang, J. Li, D. Zhao, D. Xu, Q. Gong, J. Liao, Clinical characteristics and intrauterine vertical transmission potential of COVID-19 infection in nine pregnant women: a retrospective review of medical records. *The Lancet* **395.10226** (2020), 809–815.
- [24] Y. Li, L. Xia, Coronavirus disease 2019 (COVID-19): role of chest CT in diagnosis and management. *American Journal of Roentgenology* **214.6** (2020), 1280–1286.

- [25] J. Wei, H. Xu, J. Xiong, Q. Shen, B. Fan, C. Ye, W. Dong, F. Hu, 2019 novel coronavirus (COVID-19) pneumonia: serial computed tomography findings. *Korean Journal of Radiology* **21.4** (2020), 501.
- [26] Working Group of 2019 Novel Coronavirus, Peking Union Medical College Hospital, Diagnosis and clinical management of 2019 novel coronavirus infection: an operational recommendation of Peking Union Medical College Hospital (V2.0). *Zhonghua Nei Ke Za Zhi* **59** (2020), 186–188.
- [27] T. Ozturk, M. Talo, E. A. Yildirim, U. B. Baloglu, O. Yildirim, U. R. Acharya, Automated detection of COVID-19 cases using deep neural networks with X-ray images. *Computers in Biology and Medicine* **121** (2020), 103792.
- [28] A. Makris, I. Kontopoulos, K. Tserpes, COVID-19 detection from chest X-ray images using Deep Learning and Convolutional Neural Networks. *11th Hellenic Conference on Artificial Intelligence* (2020), 60–66.
- [29] D. C. Novitasari, R. Hendradi, R. E. Caraka, Y. Rachmawati, N. Z. Fanani, A. Syarifudin, T. Toharudin, R. C. Chen, Detection of COVID-19 chest X-ray using support vector machine and convolutional neural network. *Commun. Math. Biol. Neurosci.* (2020).
- [30] C. Qin, F. Liu, T. C. Yen, X. Lan, 18 F-FDG PET/CT findings of COVID-19: a series of four highly suspected cases. *European Journal of Nuclear Medicine and Molecular Imaging* (2020), 1–6.
- [31] E. Guedj, A. Verger, S. Cammilleri, PET imaging of COVID-19: the target and the number. *European Journal of Nuclear Medicine and Molecular Imaging* **47.7** (2020), 1636–1637.
- [32] R. Amin, L. Grinblat, M. Husain, Incidental COVID-19 on PET/CT imaging. *Canadian Medical Association Journal* **192.23** (2020), E631.
- [33] D. Albano, F. Bertagna, M. Bertoli, G. Bosio, S. Lucchini, F. Motta, M. B. Panarotto, A. Peli, L. Camoni, F. M. Bengel, R. Giubbini, Incidental findings suggestive of COVID-19 in asymptomatic patients undergoing nuclear medicine procedures in a high-prevalence region. *Journal of Nuclear Medicine* **61.5** (2020), 632–636.
- [34] Big Data Technologies for Ultra-High-Speed Data Transfer in Life Sciences. *Intel* (2013).
- [35] H. Kim, A. Irimia, S. M. Hobel, M. Pogosyan, H. Tang, P. Petrosyan, R. E. Blanco, B. A. Duffy, L. Zhao, K. L. Crawford, S. L. Liew, The

- LONI QC system: a semi-automated, web-based and freely-available environment for the comprehensive quality control of neuroimaging data. *Frontiers in Neuroinformatics* **13** (2020), 60.
- [36] M. Chung, A. Bernheim, X. Mei, N. Zhang, M. Huang, X. Zeng, J. Cui, W. Xu, Y. Yang, Z. A. Fayad, A. Jacobi, CT imaging features of 2019 novel coronavirus (2019-nCoV). *Radiology* **295.1** (2020), 202–207.
- [37] J. Hofmanninger, F. Prayer, J. Pan, S. Röhrich, H. Prosch, G. Langs, Automatic lung segmentation in routine imaging is primarily a data diversity problem, not a methodology problem. *European Radiology Experimental* **4.1** (2020), 1–13.
- [38] Z. Liu, A. McClung, H. W. Yeung, Y. Y. Chung, S. M. Zandavi, Top-down person re-identification with Siamese convolutional neural networks. *2018 International Joint Conference on Neural Networks (IJCNN), IEEE* (2018), 1–8.

DOMINIQUE DUNCAN
LABORATORY OF NEURO IMAGING
USC STEVENS NEUROIMAGING AND INFORMATICS INSTITUTE
KECK SCHOOL OF MEDICINE
UNIVERSITY OF SOUTHERN CALIFORNIA
2025 ZONAL AVENUE
LOS ANGELES, CALIFORNIA
USA
E-mail address: duncand@usc.edu

RECEIVED DECEMBER 9, 2020